

Self-supervised object detection from audio-visual correspondence

Triantafyllos Afouras^{1*†} Yuki M. Asano^{1*} Francois Fagan² Andrea Vedaldi² Florian Metze²
¹ Visual Geometry Group, University of Oxford
² Facebook AI
 afourast@robots.ox.ac.uk

Abstract

We tackle the problem of learning object detectors without supervision. Differently from weakly-supervised object detection, we do not assume image-level class labels. Instead, we extract a supervisory signal from audio-visual data, using the audio component to “teach” the object detector. While this problem is related to sound source localisation, it is considerably harder because the detector must classify the objects by type, enumerate each instance of the object, and do so even when the object is silent. We tackle this problem by first designing a self-supervised framework with a contrastive objective that jointly learns to classify and localise objects. Then, without using any supervision, we simply use these self-supervised labels and boxes to train an image-based object detector. With this, we outperform previous unsupervised and weakly-supervised detectors for the task of object detection and sound source localization. We also show that we can align this detector to ground-truth classes with as little as one label per pseudo-class, and show how our method can learn to detect generic objects that go beyond instruments, such as airplanes and cats.

1. Introduction

While recent progress in learning image and video representations has been substantial [23, 34, 39, 100], this has not yet translated into an ability to learn interpretable and actionable concepts automatically. By that, we mean that some manual labels are still required in order to map unsupervised representations to useful concepts such as image classes or object detections. In this paper, we thus consider the problem of learning interpretable concepts without any manual supervision. In particular, we focus on a problem that has not been explored extensively in the literature: learning to simultaneously detect and classify objects with no manual labels at all.

*Joint first authors.

†Work done during an internship at Facebook.

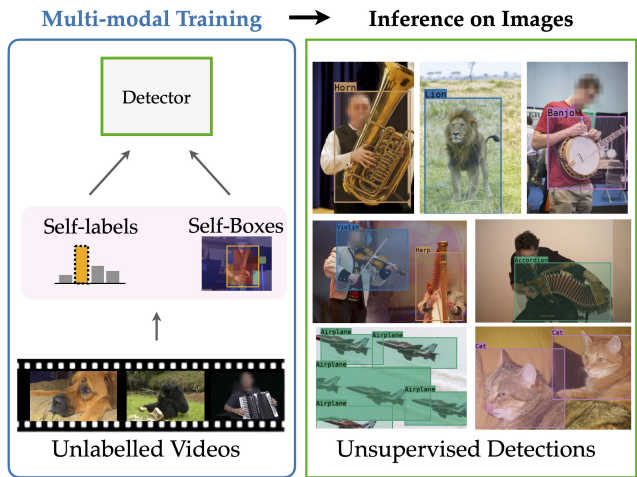


Figure 1: **We train an object detector simply by watching videos.** Without using any manual annotations, we learn to detect different objects in images, by first self-labelling boxes and object categories and then using those as targets to teach a detector. The detection results shown are outputs from our trained model; for visualisation purposes we show Hungarian-matched labels.

This problem is related to weakly supervised object detection (WSOD [16, 65]), with the difference that, in WSOD, the learning algorithm is given image-level labels telling it whether the image contains an occurrence of a given object type or not. Inspired by recent work in self-supervised learning, we seek to replace this source of external supervision with an internal supervisory signal extracted from the observation of video data. Videos are far richer than images, for example because they contain motion. Here, we focus on the multi-modal aspect of videos and use sound as a weak and noisy cue to learn about objects in the visual component of the data.

The power of multi-modal self-supervision has been demonstrated before in self-supervised representation learning, and, closely related, in *video clustering* [9]. However, while video clustering can provide an interpretation

of the data in terms of discrete classes, it does not provide any information about the location of the relevant objects in images. On the other hand, *sound source localisation* [7, 11, 52, 69] has considered precisely the problem of localizing the source of sounds in images. It is therefore tempting to trivially combine image classification and sound source localisation in the hope of learning the type and location of objects automatically.

Unfortunately, such an approach does *not* lead to a satisfactory object detector. To understand why, it is important to note that the goal of sound source localisation is to *localize the sound while it is being heard*. This is insufficient for a detector because many objects emit sounds only occasionally and they become invisible to source localisation when they are silent. Instead, a detector that works in the visual domain should be responsive even when the object cannot be heard. Furthermore, source localisation methods generally only extract a heatmap giving the distribution of possible object locations; in contrast, a detector solves the much harder problem of enumerating all individual object instances that occur in an image by outputting instance-specific bounding boxes.

In order to solve these issues, we should treat the sound component as a useful cue to *learn* an object detector, but not as a cue which is *necessary for detection*. Instead, we consider the problem of taking as input a collection of raw videos and producing a list of object classes and locations, in order to train an image-based detector.

On a high level, our method is based on the following observation: we can use a sound source localisation network to learn about possible locations of sounding objects in videos. From this, we can extract a collection of bounding box pseudo-annotations for the objects and use those to learn a standard object detector. Because the latter only uses the visual modality, it immediately transfers to the detection of objects even when no relevant sound is present.

However, one challenge is that sound source localisation does not provide the necessary class information to train class-specific detectors, effectively resulting in only learning a region proposal network for generic objects, with high rates of false positives. To this end, we note that most sound source localizers are based on noise-contrastive formulations that, together with clustering-based approaches, occupy the current state-of-the-art in self-supervised representation learning. Leveraging this, we derive a joint formulation that can simultaneously benefit from and learn to localize sound sources and classify them without *any* supervision. The resulting output can then be used to train any off-the-shelf object detector such as a Faster-RCNN [76] to obtain a completely unsupervisedly learned object detector, as shown in Fig. 1.

Empirically, we test our method by training and testing on VGGSound [21] and AudioSet [32], as well as testing

only on a subset of OpenImages [56].

2. Related Work

Audio-Visual Sound Source Localisation. Early work in sound-source localisation includes probabilistic models for localisation [27, 42, 53] and segmentation [48], but more recently the focus has shifted to dual-stream neural networks. For example, [7, 38, 82] propose a contrastive learning approach that matches the visual and audio components of the data. The work of [43, 47] instead clusters visual and audio features, associating to them centroids by means of a contrastive loss. Other works [2, 67] learn heatmaps by exploiting audio-visual synchronization in the same video, used previously for lip-to-mouth synchronization and active-speaker detection [24, 61], or by leveraging explicit attention modules [51]. Zhao et al. [108, 109] learn to associate pixels with audio sources by training with a mix-and-separate objective. Others [73] combine activation maps learned from class labels [19, 81] with a contrastive objective, use different levels of supervision and fusion techniques [74], or improve heatmaps by mining hard negative locations [20].

The work most similar to ours is [45], who first train a source localisation model with a contrastive objective and then use the learned heatmaps to extract object representations that are clustered using K-means. The cluster assignments are then used to train classifiers on top of the audio and video encoders. The paper proceeds to use these learned representations to discriminatively localize sound sources while suppressing quiet objects in ‘cocktail party’ scenarios.

Compared to our work, none of the above can detect and thus enumerate individual object occurrences because they produce heatmaps. Furthermore, they all require audio during inference, and therefore cannot be used on individual images or to detect silent objects.

Audio-visual category discovery. Learning visual categories is usually cast as image clustering, for which there is abundant prior work, such as recent ‘deep clustering’ methods [10, 18, 49, 95, 101, 103], or clustering with segmentation [97]. However, there is less work for clustering audio-visual data. In [5] the authors extend Deep Cluster [18] to the video domain by constructing two sets of labels from opposing modalities, which are used for cross-modal representation learning. The work of [80] combines clustering with audio-visual co-segmentation achieving combined audio-visual source separation. In [9], the authors extend the self-labelling method of [10] to multi-modal data by learning a shared set of labels between the two modalities. This work builds on the latter to complement and boost sound source localisation in a joint learning framework.

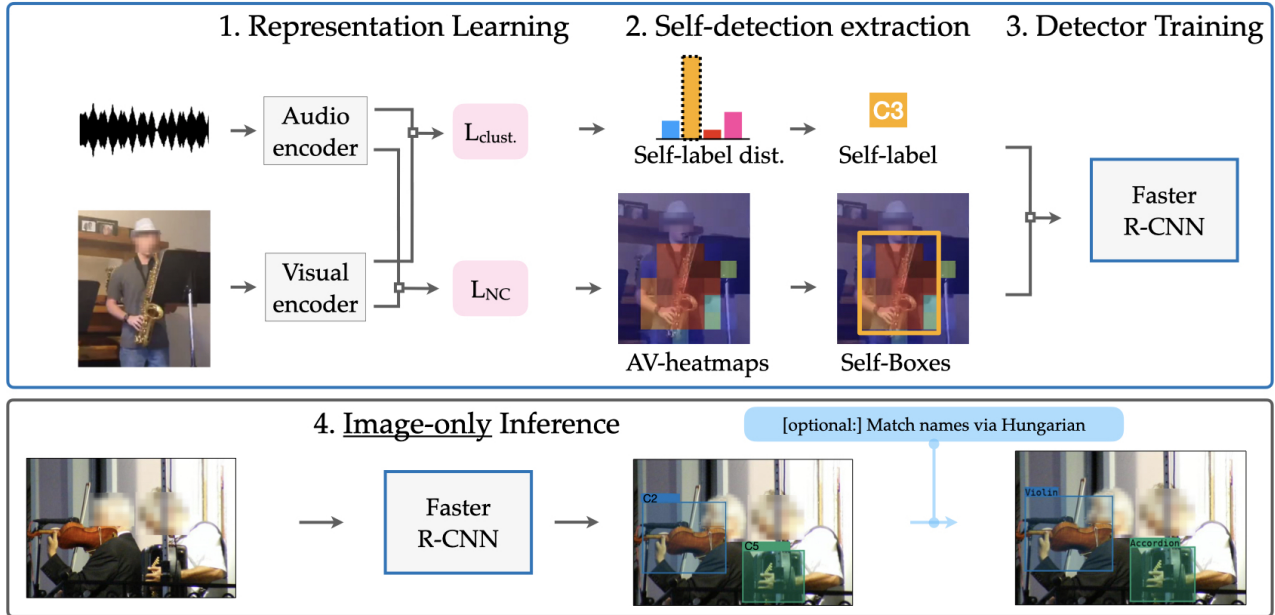


Figure 2: Self-supervised object detection from audio-visual correspondence: We combine noise-contrastive and clustering-based self-supervised learning to generate self-detections (boxes and labels) and use those as targets to train a detector. The trained detector can be used to detect objects from many categories on images without requiring audio.

Weakly Supervised Object Detection (WSOD). Weakly supervised detection uses (manual) image-level category labels without bounding box annotations. Many approaches are based on a form of multiple-instance learning [17, 33, 91, 98, 102, 104, 105, 107], or proposal clustering [90]. Recent works in the area [50, 77] combine a variety of ideas, such as self-training [112] and spatial dropout [99] or explore the use of mixed annotations [78]. Other works obtain improvements by adding curriculum learning [106], using motion cues in videos [86], adversarial training [84], combining segmentation and detection [31, 58, 83], or modelling the uncertainty of object locations [8].

Other methods use technique such as CAM or analogous techniques [15, 19, 28, 81, 85, 111] as a form of weakly supervised saliency or localisation maps. Recent works have suggested that saliency methods can also be applied to self-supervised networks [13, 35], e.g. for object co-localisation [13].

Self-supervised multi-modal learning. Our work is also related to methods that use multiple modalities for representation learning [5, 6, 10, 12, 63, 70, 71] and synchronization [25, 54, 68]. A number of recent papers have leveraged speech as a weak supervisory signal to train video representations [57, 62, 64, 87, 88] whereas [3] uses speech, audio and video. Some works distil knowledge learned from one modality into another [1, 4, 29, 110]. Other works incorporate optical flow and other modalities [36, 37, 72, 108] to learn representations. For instance, the work of [93] learns

to temporally localize audio events through audio-visual attention. CMC [92] learns representations that are invariant to multiple views of the data such as different color channels. Multi-modal self-supervision is also used to learn sound source separation in [30], albeit they assume to have pre-trained detectors.

3. Method

Our goal is to learn object detectors using only unlabeled videos, simultaneously learning to enumerate, localize and classify objects. Our approach consists of three stages summarized in Fig. 2: first, we learn useful representations using clustering and contrastive learning; second, we extract bounding boxes and class categories by combining the trained localisation and classification networks; third, we train an off-the-shelf object detector by using these self-extracted labels and boxes as targets.

Next, we explain each stage and refer the reader to the the Appendix for further architecture and training details.

3.1. Representation Learning

Sound source spatial localisation. Our method starts by training a sound source localisation network (SSLN) using a contrastive learning formulation inspired by [7]. The SSLN is learned from pairs (v, a) , where $v \in \mathbb{R}^{3 \times H \times W}$ is a video frame (i.e., a still image) and $a \in \mathbb{R}^{T \times F}$ is the spectrogram of the audio captured in a temporal window centered at that particular video frame.

We consider a pair of deep neural networks. The first network $f^v(v) \in \mathbb{R}^{C \times h \times w}$ extracts from the video frame a field of C -dimensional feature vectors, one per spatial location. We use the symbol $f_u^v(v) \in \mathbb{R}^C$ to denote the feature vector associated to location $u \in \psi = \{1, \dots, h\} \times \{1, \dots, w\}$. Here $h \times w$ is the resolution at which the spatial features are computed and is generally a fraction of the video frame resolution $H \times W$. The second network $f^a(a) \in \mathbb{R}^C$ extracts instead a feature vector for the audio signal.

Importantly, the spatial and audio features share the same C -dimensional embedding space and can thus be contrasted. We further assume that the vectors $f_u^v(v)$ and $f^a(a)$ are L^2 normalized (this is obtained by adding a normalization layer at the end of the corresponding networks). The cosine similarity of the two feature vectors is then used to compute a heatmap of spatial locations, with the expectation that objects that are correlated with the sounds would respond more strongly. This heatmap is given by:

$$h_u(v, a) = \langle f_u^v(v), f^a(a) \rangle / \rho, \quad u \in \psi,$$

where ρ , is a learnable temperature parameter.

For the multi-modal contrastive learning formulation [26, 66, 71], the heatmap is converted in an overall score that the video v and audio a are in correspondence. This is done by taking the maximum of the response:

$$S(v, a) = \max_{u \in \psi} h_u(v, a).$$

The contrastive learning objective is defined by considering videos $(v, a) \in \mathcal{B}$ in a batch \mathcal{B} . This comprises two terms. The first tests how well a video frame matches with its specific audio among the ones available in the batch:

$$\mathcal{L}_{a \rightarrow v}(\mathcal{B}) = -\frac{1}{|\mathcal{B}|} \sum_{(v, a) \in \mathcal{B}} \log \frac{\exp S(v, a)}{\sum_{(v', a') \in \mathcal{B}} \exp S(v, a')}.$$

The second is analogous, testing how well an audio matches with its specific video frame:

$$\mathcal{L}_{v \rightarrow a}(\mathcal{B}) = -\frac{1}{|\mathcal{B}|} \sum_{(v, a) \in \mathcal{B}} \log \frac{\exp S(v, a)}{\sum_{(v', a') \in \mathcal{B}} \exp S(v', a')}.$$

These two losses are averaged in the *noise-contrastive* loss:

$$\mathcal{L}_{\text{NC}}(\mathcal{B}) = (\mathcal{L}_{a \rightarrow v}(\mathcal{B}) + \mathcal{L}_{v \rightarrow a}(\mathcal{B})) / 2 \quad (1)$$

Category self-labeling. Spatial localisation does not provide any class information, whereas our goal is to also associate ‘names’ to the different objects in the dataset. To this end, we consider the self-labelling approach of [9]. To briefly explain the formulation, let $y(v, a) \in \mathcal{Y} = \{1, \dots, K\}$ be a label associated to the training pair (v, a) .

We also consider two classification networks. The first maps a video v to class scores $g^v(v) \in \mathbb{R}^K$ and is optimized by minimizing the standard cross-entropy loss:

$$\mathcal{L}_v(\mathcal{B}|y) = -\frac{1}{|\mathcal{B}|} \sum_{(v, a) \in \mathcal{B}} \log \text{softmax}(y(v, a) | g^v(v)).$$

Note that this classification loss is equivalent to a contrastive loss on the cluster indices (as opposed to image indices) without normalization: As the last classification layer can be viewed as computing dot-products with each corresponding cluster’s feature, it pushes the representation towards the feature of the corresponding cluster and away from the other clusters. The other network $g^a(a)$ is analogous, but uses the audio signal:

$$\mathcal{L}_a(\mathcal{B}|y) = -\frac{1}{|\mathcal{B}|} \sum_{(v, a) \in \mathcal{B}} \log \text{softmax}(y(v, a) | g^a(a)).$$

As noted in [9], the crucial link between the two losses is that the labels y are shared between modalities. This is obtained by averaging the two losses:

$$\mathcal{L}_{\text{clust}}(\mathcal{B}|y) = (\mathcal{L}_v(\mathcal{B}|y) + \mathcal{L}_a(\mathcal{B}|y)) / 2. \quad (2)$$

Note that the labels y are unknown; following [9] these are learned in an alternate fashion with the classification networks, minimizing the same loss (2). In order to avoid degenerate solutions, the labels’ marginal distribution must be specified, e.g. using a simple equipartitioning constraint:

$$\frac{1}{|\mathcal{D}|} \sum_{(v, a) \in \mathcal{D}} 1_{\{y(v, a) = k\}} = \frac{1}{K} \quad \text{for all } k = 1, \dots, K \quad (3)$$

where \mathcal{D} denotes the entire dataset (union of all batches). Optimizing y can be done efficiently by using the SK algorithm as in [9].

Joint training. To summarize, given the dataset \mathcal{D} , we optimize stochastically w.r.t. random batches \mathcal{B} the loss:

$$\mathcal{L}(\mathcal{B}|y) = \lambda \mathcal{L}_{\text{NC}}(\mathcal{B}) + (1 - \lambda) \mathcal{L}_{\text{clust}}(\mathcal{B}|y) \quad (4)$$

where λ is a balancing hyperparameter.

The loss is optimized with respect to the localisation networks f^v and f^a and the classification networks g^v and g^a . These networks share common backbones q^v and q^a and differ only in their heads, so they can be written as $f^v = \hat{f}^v \circ q^v$, $g^v = \hat{g}^v \circ q^v$, $f^a = \hat{f}^a \circ q^a$ and $g^a = \hat{g}^a \circ q^a$.

The model is trained by alternating between updating the labels y with eq. (2) under constraint (3) and updating the networks by optimizing eq. (4).

3.2. Extraction of Self-labels for Detection

Once the localisation and classification networks have been trained, they can be used to extract self-annotations for training a detector. This is done in two steps: extracting object bounding boxes and finding their class labels.

Box extraction. To obtain “self-bounding boxes” for the objects, we use the simple heuristic suggested by [111]: the heatmap $h(v, a)$ is thresholded at a value $\epsilon(h)$, the largest connected component is identified, and a tight bounding box $t^*(v, a) \in \Omega^2$ around that component is extracted (the notation means that the box is specified by the location of the top-left and bottom-right corners).

The threshold is determined dynamically as a convex combination of the maximum and average responses of the heatmap, controlled by hyperparameter β :

$$\epsilon(h) = \beta \max_{u \in \psi} h_u + (1 - \beta) \frac{1}{|\psi|} \sum_{u \in \psi} h_u. \quad (5)$$

Class labelling. As noted above, we only extract a single object from each frame for the purpose of training the detector. Likewise, we only need to extract a single class label for the frame. This is done by taking the maximum response of the visual and audio-based classification networks:

$$y^*(v, a) = \arg \max_{y \in \mathcal{Y}} [g_y^v(v) + g_y^a(a)]. \quad (6)$$

Filtering the annotations. The assumption that frames contain a dominant object introduces noise but simplifies the problem and gives us the ability to use the audio to obtain purer clusters. Notably, we do not require the method above to work for *all* frames but instead rely on our detector to smooth over the specific and noisy self-annotations to learn a holistic detection.

3.3. Training the Object Detector

The process described above results in a shortlist of training triplets $(v, t^*, y^*) \in \mathcal{D}_{\text{det}}$, where v is a video frame (an image), t^* is the extracted bounding box and y^* is its class label. We use this dataset to train an off-the-shelf detector, in particular Faster R-CNN [75] for its good compromise between speed and quality.

Recall that, given an image v , Faster R-CNN detector considers a set of bounding box proposals $m \in M(v) \subset \Omega^2$. It then trains networks $y(m) = f_{\text{det}}^{\text{cls}}(m|v) \in \{1, \dots, K, \text{bkg}\}$ and $t(m) = f_{\text{det}}^{\text{loc}}(m|v) \in \mathbb{R}^4$ inferring, respectively, the class label $y(m)$ and a refined full-resolution bounding box $t(m)$ for the box proposal m . The label space is extended to also include a *background class* bkg , which is required as most proposals do not land on any object.

The detector is trained by finding an association between proposals and annotations. To this end, if $m^* = \arg \max_{m \in M(v)} \text{IoU}(m, t^*)$ is the proposal that matches the pseudo-ground truth bounding box t^* the best, one optimizes:

$$\begin{aligned} \mathcal{L}_{\text{det}}(v, t^*, y^*) &= \mathcal{L}_{\text{reg}}(t(m^*), t^*) + \mathcal{L}_{\text{cls}}(y(m^*), y^*) \\ &+ \sum_{m \in M(v): \text{IoU}(m, t^*) < \tau} \mathcal{L}_{\text{cls}}(y(m), \text{bkg}). \end{aligned}$$

Here \mathcal{L}_{reg} is the L^1 loss for the bounding box corner coordinates and \mathcal{L}_{cls} the standard cross-entropy loss. Intuitively, this loss requires the best proposal m^* to match the pseudo-ground truth class y^* and bounding box t^* of, while mapping proposal m that are a bad match ($\tau \leq 0.7$) to class bkg . Further details, including how the region-proposal network that generates the proposals is trained, are given in the the Appendix

Discussion. Training a detector is obviously necessary to solve the problem we set out to address. However, it can also be seen as a way of extracting ‘clean’ information from the noisy self-annotations. Specifically: (i) the noise in individual annotations is smoothed over the entire dataset; (ii) because of the built-in NMS step, the detector still learns to extract multiple objects per image even though a single self-annotation is given for each training image; (iii) by learning to reject a large number of false bounding box proposals, the detector learns to be more precise than the self-annotations are.

4. Experiments

We first introduce the datasets, experimental setup and relevant baselines; we then test our method against those, analyse it further via ablations and its capacity to generalize.

4.1. Datasets

AudioSet-Instrument. AudioSet [32] is a large scale audio-visual dataset consisting of 10-second video clips originally from YouTube. For training we use the *AudioSet-Instruments* [7] subset of the “unbalanced” split, containing 110 sound source classes as well as its more constrained subset used by [45] spanning 13 instrument classes. Following previous work we use the “balanced” subset for evaluation on the annotations provided by [45].

VGGSound. VGGSound contains over 200K 10-second clips from YouTube spanning 309 categories of objects where there is some degree of correlation between the audio and the video. We create one subset by keeping only the 50 musical instrument categories yielding around 54K training videos, and one other subset, by keeping from those only the 39 categories that can be roughly mapped to the test-set annotations (details in the Appendix). For VGGSound pseudo-ground truth test-set annotations are obtained using a supervised detector from [30], following [45].

OpenImages. For evaluation, we also use the subset of the OpenImages [56] dataset containing musical instruments, which spans 15 classes.

4.2. Baselines

We are not aware of any prior work that learns an object detector for multiple object classes without any supervision. Instead, we compare against weakly-supervised detectors

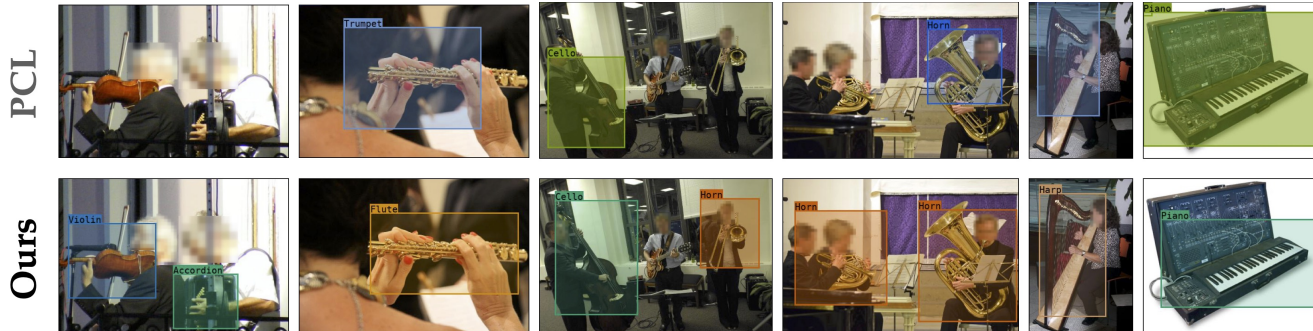


Figure 3: **Qualitative results and comparison** with a weakly supervised object detection method, PCL [90], on the Open-Images test set. Our method accurately detects objects, capturing their boundaries, even though it has been trained without *any* supervision. For visualisation purposes, we show the labels obtained from matching with the Hungarian method. More qualitative results provided in the the Appendix.

(hence using image-level labels) and unsupervised localisation methods that only produce heatmaps (not detections).

Weakly-supervised detection. For weakly-supervised detection, we consider PCL [89], the strongest such baseline for which we could find an implementation. Image-level labels are obtained from the corresponding dataset: for AudioSet the 13 labels of the training set are used, and for VGGSound we manually merge the 39 sub-classes to equivalent 15 classes (e.g., electric guitar, acoustic guitar to “Guitar” etc.); see the Appendix for full details. However, we have found that training PCL directly on the same data as our method (i.e., random clips from the VGGSound and AudioSet-Instrument subsets) does not work, likely due to the high amount of noise present in the labels (e.g., several videos are be labelled with an instrument, which is however not visible at all). To avoid this issue, we further preprocess the training data with a supervised instrument detector [30] and only retain frames where at least one relevant detection is found. This of course gives an “unfair” advantage to the baseline, but it is necessary to be able to use it at all.

Heatmap-based localisation. For our second baseline, we consider localisation methods that, similarly to us, use cross-modal self-supervised learning. The state-of-the-art DSOL method of [45] is the most relevant, as it produces a heatmap roughly localizing the objects and produces class pseudolabels. While DSOL does not use image-level labels like PCL, it does use audio during inference, and thus strictly more information than our method (which performs localisation only in the visual domain).

Region proposals. Finally, we also compare against other baselines such as simply predicting a large centered box and class-agnostic region proposal methods such as selective search, and using a RPN obtained from supervised training on COCO [59].

4.3. Implementation Details.

Assessing class pseudolabels. Since class pseudolabels do not come with the “name” of the class (they are just cluster indices), they must be put in correspondence with human-labelled classes for evaluation. Following prior work in unsupervised image clustering [10, 14, 49, 96], we apply Hungarian matching [55] to the learned clusters and the ground truth classes. Importantly, the matching is done *after* the detector is trained and only done for assessment; meaning that the detector does not use any manual label.

Training resolutions. We train our method on random square crops of 224 pixels after resizing to 256 pixels. During the training of the detector, we take random 224 crops and obtain the the self-supervised bounding boxes on-the-fly from our pretrained model, which are scaled and used to train the detector at the larger detector resolution.

Detector warm-up. We warm-up the Faster R-CNN detector by training in a class-agnostic manner for 20 epochs. This gives the RPN (which is randomly initialized) an opportunity to learn sufficiently stable bounding box proposals; we then switch to full class-aware supervision. We found that this leads to more robust convergence compared to training with pseudo-labels from the start.

Backbone pretraining. We also found it beneficial to pretrain the localizer backbone using only the localisation loss on the full AudioSet-Instruments dataset, and the detector backbone using self-supervised SimCLR [22] on ImageNet (note that the DSOL baseline uses instead *supervised* ImageNet pretraining for the backbone).

Detector training. If not stated otherwise, the localizer and detector are trained on VGGSound and AudioSet whereas OpenImages are only used for evaluation. We do not have any information on the number of instruments in VGGSound and use all videos with no single/multi-object curation. For a fair comparison with DSOL, and only for

Method	No labels?	VGGSound			Audioset			OpenImages		
		mAP ₃₀	mAP ₅₀	mAP _[50:95:5]	mAP ₃₀	mAP ₅₀	mAP _[50:95:5]	mAP ₃₀	mAP ₅₀	mAP _[50:95:5]
PCL (WSOD) [90]	✗	54.9	27.7	7.6	39.0	17.5	4.4	37.9	14.5	3.5
Ours - weak sup.	✗	67.6	42.9	14.2	50.6	30.9	10.3	48.9	33.7	9.5
Center Box*	✓	29.6	5.6	1.5	15.1	3.5	0.7	20.7	4.2	0.8
Selective Search* [94]	✓	5.2	1.1	0.4	2.8	0.4	0.1	7.4	2.1	0.7
COCO-trained RPN*	✗	33.4	7.5	1.6	19.0	4.1	0.8	24.4	11.1	2.6
Ours - self-boxes*	✓	48.1	29.6	10.0	27.8	14.1	4.8	NA	NA	NA
Ours - full	✓	52.3	39.4	14.7	44.3	28.0	9.6	39.9	28.5	7.6

Table 1: **Self-supervised object detection.** We report object detection metrics across three test datasets and find our method is far superior to other unsupervised approaches and outperforms even the weakly supervised baseline in most metrics. For methods denoted by *, we report class-agnostic evaluation numbers. *Center Box* denotes a simple baseline predicting random sized boxes in the middle of the frame. *Ours-weak sup.* is a variant of our model trained with the video-level category annotations in combination with our self-extracted boxes. The class-agnostic performance of the self-boxes that are used to train the detector reveals that the latter greatly outperforms them, which highlights the benefit of our approach.

Method	single-instr.		multi-instr.
	IoU-0.5	AUC	cIoU-0.3
Sound of pixels [109]	38.2	40.6	39.8
Object t. Sound [7]	32.7	39.5	27.1
Attention [82]	36.5	39.5	29.9
DMC [44]	32.8	38.2	32.0
DSOL [45]	38.9	40.9	48.7
Ours	50.6	47.5	52.4

Table 2: **Comparison to sound localisation methods.** Since our detector does not require audio, we obtain detections on the video frames directly. Our model outperforms the baselines. Baselines numbers taken from [46].

the relevant experiment in Table 2, we train on AudioSet using the single-instrument subset for learning the localizer.

Number of clusters. For VGGSound training we use $K = 39$ if not stated otherwise, matching the 39 object types in the training set. Since the dataset is roughly balanced, uniform marginals are used as described in [9]. For AudioSet training we use $K = 30$ and Gaussian marginals.

4.4. Results

Self-supervised object detection. We summarise the results of our evaluations on the three test sets that we consider in Table 1. Following the image object detection literature, we use mAP at different IOU thresholds as the evaluation metric.

Our method clearly outperforms the PCL baseline even though it uses no manual annotations at all during training. PCL outperforms our approach in some of the datasets only if the IoU threshold used for mAP computation is relaxed

substantially (0.3 IoU). However, for stricter thresholds our approach works better, which suggests that our detections have a relatively high spatial accuracy.

To understand the impact of the noisy class self-labels, we also train and test a detector (Ours - weak sup.) with the bounding box labels from our localisation network, but utilising the ground truth video categories. The resulting performance difference is modest, resulting in a 3% AP50 drop in VGGSound and AudioSet. This further demonstrates the accuracy of our class self-labels, but also shows that our method has also the potential to leverage weak supervision if available.

Per-class performance breakdown. To better understand the strengths and weaknesses of our method, we report a performance breakdown by object class in Table 3. We observe that the model obtains good results consistently for classes of large objects with a distinctive appearance (e.g. accordions and harps), while it is weaker for smaller objects such as oboes, or for objects that appear closely in numbers, like drums.

Comparison to audio-visual heatmaps. In Table 2 we compare the performance of our method trained on AudioSet to state-of-the-art sound source localisation methods. For a fair comparison to these methods, we convert the union of our predicted bounding boxes with confidence above a set threshold into a binary map, and use the latter as a pseudo-heatmap to use the same evaluation code. Our approach outperform others for both class-agnostic single object localisation and for class-aware multi-object localisation, *without* using audio signals during inference.

We note however that cIOU is not a very reliable metric for evaluating a detector (or even sound localizer) as it favours high recall over precision: by averaging this metric over all classes the most frequent ones (e.g. drums, guitars,

Dataset	mAP ₅₀	Accordion	Cello	Drum	Flute	Horn	Guitar	Harp	Piano	Saxophone	Violin	Banjo	Trombone	Trumpet	Oboe
OpenImages	28.5	75.3	30.2	6.6	6.5	15.0	14.5	80.4	28.8	22.5	28.8	57.0	9.7	18.1	6.3
Audioset	28.0	41.3	44.9	0.9	5.5	21.7	39.5	82.6	52.7	2.5	17.4	46.7	8.0	-	-
VGGSound	39.4	88.6	39.4	1.8	50.0	3.4	34.9	95.6	50.2	14.4	56.3	100.0	2.2	11.0	3.8

Table 3: **Per-class mAP breakdown** For entries with ‘-’ the test set does not contain any samples for that class.

β	#boxes	mAP ₅₀	
		VGGS	O.Images
0.7	single	39.4	28.5
0.8	single	36.6	29.4
0.9	single	35.8	28.8
0.7-0.9	single	37.5	29.4
0.7-0.9	multi	38.0	29.3

Table 4: **Ablation of hyperparameter β** , which controls the relative width of the bounding box; *multi* denotes the use of multiple self-labelled boxes per sample. Overall the method is fairly stable with respect to the choice of this parameter, however sampling β from a range (0.7-0.9) obtains a better balanced performance. Moreover we do not observe any substantial improvement from using multiple boxes.

# GT-cls.	K	mAP ₅₀		Matching	mAP ₅₀	
		VGGS	O.Images		VGGS	O.Images
39	20	34.4	24.4	Hung.	39.4	28.5
39	30	35.1	25.1	Argmax	39.6	30.1
39	39	39.4	28.5	Manual	41.0	29.5
39	50	41.0	27.5	1-shot	36.4	25.1
				10-shot	37.1	25.8

Table 5: **Number of clusters K**. Our method is relatively robust (< 5% decrease in detection AP) to the number of clusters used for self-labelling.

Table 6: **Matching strategies**. Even with as little as 39 labels, our method can detect and classify objects accurately.

pianos) dominate the metric. We therefore propose to the research community – and report in this paper – mean average precision (mAP) values as a more indicative metric.

Ablation: Thresholding parameter. In Table 4 we investigate the influence of the hyper-parameter β and the number of extracted target boxes we use for training the detector. From Eq. (5), a smaller β makes the heatmaps more focused and specific. With regards to this parameter, we find somewhat inverse trends for VGGSound vs OpenImages, where smaller β yields better results for the former and larger β for the latter. We find that a good balance in terms of performance can be achieved by sampling β randomly from a range, as over-specific boxes for some images and under-specific ones are successfully combined during detector training. Even when extracting multiple boxes for training the detector, we find our method performs similarly

well to when only extracting a single box.

Ablation: Number of clusters K. In Table 5, we perform an experiment varying the number of clusters, and as a consequence the number of object categories that the detector learns, while keeping the test-set (containing 15 classes) fixed. We observe that our method achieves reasonable performance for a wide range of the number of clusters. The performance is fairly stable when using more clusters than the ground truth classes, and gradually decreases when fewer clusters are used.

Data-efficient detector alignment. In Table 6 we conduct an investigation into the matching of the clusters to the ground truth labels. First, we compare Hungarian matching to simply taking the argmax of the ground truth class per self-label (i.e. assigning to the most frequent class). We find this yields almost the same results for VGGSound and a gain of 1.6% on OpenImages. By refining the Hungarian assignments via manually grouping similar classes and mapping each group to one of the test classes (for example mapping ‘piano’, ‘electronic organ’ and ‘Hammond organ’ all to ‘piano’; see the Appendix for details), we find another small additional gain can be realized. While the Hungarian and argmax are common evaluation methods for the self-supervised clustering domain, we note that they are unsatisfactory as they still implicitly require a large set of labels. To alleviate this, we devise a “data-efficient” class-matching procedure as follows: Per pseudo-class, obtain the m videos which have the highest response for being in that particular pseudo-class (averaged across audio and video) and obtain the class-label for these m samples. The pseudo-class is then assigned the most frequent ground truth class among these m . Overall, this reduces the number of labels required down to Km , making it a more realistic and scalable evaluation method for self-supervised approaches. Following this procedure, we find that even by just using $m = 1$ (i.e., a total number of 39 annotations), our method still achieves high performances of 37.1% and 25.3% on VGGSound and OpenImages. This 3% drop compared to the Hungarian can be further decreased to around 2.3% by using 10 labels per pseudo-class, for a total labelling budget of 390 images.

Qualitative analysis. We show examples of successfully detected objects in challenging images in Fig. 3, where we also include the outputs of the PCL baseline. Although our model has not been manually shown any objects boundaries during training we see that it can learn very accurate boxes around them and that it can successfully identify multiple

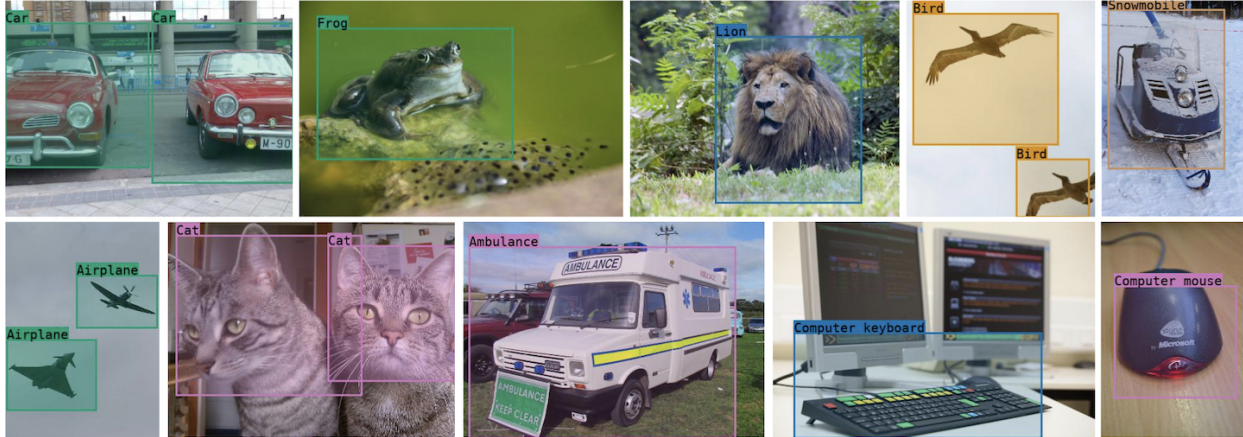


Figure 4: **Object detection beyond musical instruments.** Our proposed method can learn to accurately detect objects from more general categories, as long as they can be associated with a characteristic sound. The results shown here are from a model trained without labels directly on the full VGGSound dataset which includes 309 different video classes. Our method successfully learns to detect non-instrument objects, even in difficult multi-instance cases.

objects in complicated scenes. We provide further examples in the Appendix.

4.5. Towards general object detection

The results presented thus far have focused on subsets of common datasets with instruments solely to ensure comparability with prior works. Since one main goal of self-supervised learning is to leverage the vast amount of unlabelled data, we wish to investigate how general and robust our proposed method when applied on a far larger scale. For this, we increase our pretraining dataset by approximately $10\times$, simply by taking the whole of the VGGSound dataset, without any filtering. We set the number of learned clusters K to 300 and keep all training parameters the same; the result is an unsupervisedly trained object detector that can classify 300 pseudo-classes. As before, we match these to the VGGSound labels with the Hungarian algorithm and out of these take ten categories for which we have annotations in the OpenImages dataset (details in the Appendix).

Class	AP ₃₀	AP ₅₀	AP _[50:95:5]
Mean	45.6	24.4	6.5
Airplane	62.7	27.0	6.5
Ambulance	56.9	30.9	7.1
Bird	26.5	15.8	3.7
Car	29.8	18.4	5.1
Cat	67.7	28.0	7.7
Comp. Keyboard.	53.3	42.6	12.9
Comp. Mouse	35.9	25.4	8.8
Frog	43.5	19.5	4.7
Lion	34.1	22.2	4.9
Snowmobile	64.3	14.3	3.5

Table 7: **Results on general object categories.**

In Fig. 4 we show qualitative results of some detections on OpenImages. The numerical results are given

in Table 7. We find that even for objects that are deformable, such as cats, we get high AP₃₀ values of 67.7% and that even objects that vary in shape, such as airplanes (see Fig. 4, bottom-right), we achieve a good performances 62.7%. While the results for the AP_{50:95:5} metric indicate that there is still room for improvement, these initial results show that leveraging larger and more diverse video datasets for self-supervisedly learning object detectors is a promising avenue. We note that, since minimal curation is performed on the training data, and we use a large number of different object categories in a noisy dataset, this training setting is very challenging. These results further highlight the potential of our proposed method.

5. Conclusion

We have presented a method for training strong object detectors purely with self-supervision by watching unlabelled videos. We demonstrated that our best models perform better than a weakly supervised baseline, even after curating the dataset to filter out noisy samples for training the latter. Our method also outperforms heatmap-based methods in music instruments localisation, while having the ability to detect objects in images directly without requiring audio. We have also addressed one short-coming of using the Hungarian for evaluation by showing that data-efficient alignment of self-supervised detectors is possible with as little as one image per pseudo-label. Finally we applied our method to domains beyond musical instruments and found that it can learn reasonable detectors in this much less curated setting, paving the way to general self-supervised object detection.

Sound is a great natural source of supervision for training detectors; we believe our method will be the first of many to explore this exciting new direction.

References

- [1] Triantafyllos Afouras, Joon Son Chung, and Andrew Zisserman. ASR is all you need: Cross-modal distillation for lip reading. In *International Conference on Acoustics, Speech, and Signal Processing*, 2020. 3
- [2] Triantafyllos Afouras, Andrew Owens, Joon Son Chung, and Andrew Zisserman. Self-supervised learning of audio-visual objects from video. In *Proc. ECCV*, 2020. 2
- [3] Jean-Baptiste Alayrac, Adrià Recasens, Rosalia Schneider, Relja Arandjelovic, Jason Ramapuram, Jeffrey De Fauw, Lucas Smaira, Sander Dieleman, and Andrew Zisserman. Self-supervised multimodal versatile networks. In *Proc. NeurIPS*, 2020. 3
- [4] Samuel Albanie, Arsha Nagrani, Andrea Vedaldi, and Andrew Zisserman. Emotion recognition in speech using cross-modal transfer in the wild. In *Proc. ACMM*, 2018. 3
- [5] Humam Alwassel, Dhruv Mahajan, Bruno Korbar, Lorenzo Torresani, Bernard Ghanem, and Du Tran. Self-supervised learning by cross-modal audio-video clustering. In *Advances in Neural Information Processing Systems (NeurIPS)*, 2020. 2, 3
- [6] Relja Arandjelovic and Andrew Zisserman. Look, listen and learn. In *Proc. ICCV*, 2017. 3
- [7] Relja Arandjelovic and Andrew Zisserman. Objects that sound. In *Proc. ECCV*, 2018. 2, 3, 5, 7, 14
- [8] Aditya Arun, C. V. Jawahar, and M. Pawan Kumar. Dissimilarity coefficient based weakly supervised object detection. In *CVPR*, 2019. 3
- [9] Yuki M. Asano, Mandela Patrick, Christian Rupprecht, and Andrea Vedaldi. Labelling unlabelled videos from scratch with multi-modal self-supervision. In *Proceedings of Advances in Neural Information Processing Systems (NeurIPS)*, 2020. 1, 2, 4, 7
- [10] Yuki M. Asano, Christian Rupprecht, and Andrea Vedaldi. Self-labelling via simultaneous clustering and representation learning. In *Proceedings of the International Conference on Learning Representations (ICLR)*, 2020. 2, 3, 6
- [11] Yusuf Aytar, Carl Vondrick, and Antonio Torralba. SoundNet: Learning sound representations from unlabeled video. In *Proc. NeurIPS*, 2016. 2
- [12] Yusuf Aytar, Carl Vondrick, and Antonio Torralba. Soundnet: Learning sound representations from unlabeled video. In *Advances in Neural Information Processing Systems*, 2016. 3
- [13] Kyungjune Baek, Minhyun Lee, and Hyunjung Shim. Psynet: Self-supervised approach to object localization using point symmetric transformation. In *Proc. AAAI*, 2020. 3
- [14] Miguel A Bautista, Artsiom Sanakoyeu, Ekaterina Tikhoncheva, and Bjorn Ommer. Cliqecnn: Deep unsupervised exemplar learning. In *NeurIPS*, pages 3846–3854, 2016. 6
- [15] Loris Bazzani, Alessandra Bergamo, Dragomir Anguelov, and Lorenzo Torresani. Self-taught object localization with deep networks. In *2016 IEEE winter conference on applications of computer vision (WACV)*, pages 1–9. IEEE, 2016. 3
- [16] Hakan Bilen, Vinay P. Nambodiri, and Luc Van Gool. Object and action classification with latent variables. In *Proc. BMVC*, 2011. 1
- [17] Hakan Bilen and Andrea Vedaldi. Weakly supervised deep detection networks. In *Proceedings of the IEEE Conference on Computer Vision and Pattern Recognition (CVPR)*, 2016. 3
- [18] Mathilde Caron, Piotr Bojanowski, Armand Joulin, and Matthijs Douze. Deep clustering for unsupervised learning of visual features. In *ECCV*, 2018. 2
- [19] Aditya Chattopadhyay, Anirban Sarkar, Prantik Howlader, and Vineeth N Balasubramanian. Grad-cam++: Generalized gradient-based visual explanations for deep convolutional networks. In *2018 IEEE Winter Conference on Applications of Computer Vision (WACV)*, pages 839–847. IEEE, 2018. 2, 3
- [20] Honglie Chen, Weidi Xie, Triantafyllos Afouras, Arsha Nagrani, Andrea Vedaldi, and Andrew Zisserman. Localizing visual sounds the hard way, 2021. 2
- [21] Honglie Chen, Weidi Xie, Andrea Vedaldi, and Andrew Zisserman. VGGSound: A large-scale audio-visual dataset. In *International Conference on Acoustics, Speech, and Signal Processing (ICASS)*, 2020. 2
- [22] Ting Chen, Simon Kornblith, Mohammad Norouzi, and Geoffrey Hinton. A simple framework for contrastive learning of visual representations. *ICML*, 2020. 6, 14
- [23] Ting Chen, Simon Kornblith, Mohammad Norouzi, and Geoffrey E. Hinton. A simple framework for contrastive learning of visual representations. *arXiv.cs*, abs/2002.05709, 2020. 1
- [24] Joon Son Chung and Andrew Zisserman. Lip reading in the wild. In *Proc. ACCV*, 2016. 2
- [25] Joon Son Chung and Andrew Zisserman. Out of time: Automated lip sync in the wild. In *ACCV Workshop on Multi-view Lip-reading*, 2016. 3
- [26] Soo-Whan Chung, Joon Son Chung, and Hong-Goo Kang. Perfect match: Improved cross-modal embeddings for audio-visual synchronisation. In *Proc. ICASSP*, pages 3965–3969. IEEE, 2019. 4
- [27] John W Fisher III, Trevor Darrell, William T Freeman, and Paul A Viola. Learning joint statistical models for audio-visual fusion and segregation. In *NeurIPS*, 2000. 2
- [28] Ruth Fong and Andrea Vedaldi. Explanations for attributing deep neural network predictions. In *Proc. ICCV*, 2019. 3
- [29] Chuang Gan, Hang Zhao, Peihao Chen, David Cox, and Antonio Torralba. Self-supervised moving vehicle tracking with stereo sound. In *iccv*, 2019. 3
- [30] Ruohan Gao and Kristen Grauman. Co-separating sounds of visual objects. In *Proc. ICCV*, 2019. 3, 5, 6, 15
- [31] Weifeng Ge, Sibe Yang, and Yizhou Yu. Multi-evidence filtering and fusion for multi-label classification, object detection and semantic segmentation based on weakly supervised learning. In *CVPR*, 2018. 3
- [32] Jort F. Gemmeke, Daniel P. W. Ellis, Dylan Freedman, Aren Jansen, Wade Lawrence, R. Channing Moore, Manoj Plakal, and Marvin Ritter. Audio set: An ontology and human-labeled dataset for audio events. In *Proc. ICASSP*, 2017. 2, 5
- [33] Nicolas Gonthier, Yann Gousseau, Said Ladjal, and Olivier Bonfait. Weakly supervised object detection in artworks.

- Computer Vision – ECCV 2018 Workshops*, page 692–709, 2019. 3
- [34] Jean-Bastien Grill, Florian Strub, Florent Althé, Corentin Tallec, Pierre H. Richemond, Elena Buchatskaya, Carl Dorsch, Bernardo Ávila Pires, Zhaohan Daniel Guo, Mohammad Gheshlaghi Azar, Bilal Piot, Koray Kavukcuoglu, Rémi Munos, and Michal Valko. Bootstrap your own latent: A new approach to self-supervised learning. *CoRR*, abs/2006.07733, 2020. 1
- [35] Shir Gur, Ameen Ali, and Lior Wolf. Visualization of supervised and self-supervised neural networks via attribution guided factorization, 2020. 3
- [36] Tengda Han, Weidi Xie, and Andrew Zisserman. Memory-augmented dense predictive coding for video representation learning. In *Proc. ECCV*, 2020. 3
- [37] Tengda Han, Weidi Xie, and Andrew Zisserman. Self-supervised co-training for video representation learning. In *Proc. NeurIPS*, 2020. 3
- [38] David Harwath, Adria Recasens, Dídac Surís, Galen Chuang, Antonio Torralba, and James Glass. Jointly discovering visual objects and spoken words from raw sensory input. In *Proceedings of the European conference on computer vision (ECCV)*, pages 649–665, 2018. 2
- [39] Kaiming He, Haoqi Fan, Yuxin Wu, Saining Xie, and Ross B. Girshick. Momentum contrast for unsupervised visual representation learning. *arXiv.cs*, abs/1911.05722, 2019. 1
- [40] Kaiming He, Georgia Gkioxari, Piotr Dollár, and Ross B. Girshick. Mask R-CNN. In *Proc. ICCV*, 2017. 14
- [41] Kaiming He, Xiangyu Zhang, Shaoqing Ren, and Jian Sun. Deep residual learning for image recognition. *arXiv preprint arXiv:1512.03385*, 2015. 14
- [42] J Hershey and JR Movellan. Audio-vision: Locating sounds via audio-visual synchrony. In *NeurIPS*, volume 12, 1999. 2
- [43] Di Hu, Feiping Nie, and Xuelong Li. Deep multimodal clustering for unsupervised audiovisual learning. In *Proceedings of the IEEE/CVF Conference on Computer Vision and Pattern Recognition (CVPR)*, June 2019. 2
- [44] Di Hu, Feiping Nie, and Xuelong Li. Deep multimodal clustering for unsupervised audiovisual learning. In *Proc. CVPR*, 2019. 7
- [45] Di Hu, Rui Qian, Minyue Jiang, Xiao Tan, Shilei Wen, Errui Ding, Weiyao Lin, and Dejing Dou. Discriminative sounding objects localization via self-supervised audiovisual matching. In *NeurIPS*, 2020. 2, 5, 6, 7
- [46] Di Hu, Rui Qian, Minyue Jiang, Xiao Tan, Shilei Wen, Errui Ding, Weiyao Lin, and Dejing Dou. Discriminative sounding objects localization via self-supervised audiovisual matching. *arXiv.cs*, abs/2010.05466, 2020. 7
- [47] Di Hu, Zongge Wang, Haoyi Xiong, Dong Wang, Feiping Nie, and Dejing Dou. Curriculum audiovisual learning. *ArXiv*, abs/2001.09414, 2020. 2
- [48] Hamid Izadinia, Imran Saleemi, and Mubarak Shah. Multimodal analysis for identification and segmentation of moving-sounding objects. *IEEE Transactions on Multimedia*, 15(2):378–390, 2012. 2
- [49] Xu Ji, João F Henriques, and Andrea Vedaldi. Invariant information clustering for unsupervised image classification and segmentation. In *Proceedings of the IEEE International Conference on Computer Vision*, pages 9865–9874, 2019. 2, 6
- [50] Zequn Jie, Yunchao Wei, Xiaojie Jin, Jiashi Feng, and Wei Liu. Deep self-taught learning for weakly supervised object localization. In *CVPR*, 2017. 3
- [51] Naji Khosravan, Shervin Ardeshtir, and Rohit Puri. On attention modules for audio-visual synchronization. *arXiv preprint arXiv:1812.06071*, 1, 2018. 2
- [52] Einat Kidron, Yoav Y. Schechner, and Michael Elad. Pixels that sound. In *Proc. CVPR*, 2005. 2
- [53] Einat Kidron, Yoav Y Schechner, and Michael Elad. Pixels that sound. In *Proc. CVPR*, 2005. 2
- [54] Bruno Korbar, Du Tran, and Lorenzo Torresani. Co-operative learning of audio and video models from self-supervised synchronization. 2018. 3
- [55] Harold W Kuhn. The hungarian method for the assignment problem. *Naval research logistics quarterly*, 2(1-2):83–97, 1955. 6
- [56] Alina Kuznetsova, Hassan Rom, Neil Alldrin, Jasper Uijlings, Ivan Krasin, Jordi Pont-Tuset, Shahab Kamali, Stefan Popov, Matteo Mallocci, Tom Duerig, et al. The open images dataset v4: Unified image classification, object detection, and visual relationship detection at scale. *arXiv preprint arXiv:1811.00982*, 2018. 2, 5
- [57] Tianhao Li and Limin Wang. Learning spatiotemporal features via video and text pair discrimination. *arXiv.cs*, abs/2001.05691, 2020. 3
- [58] Xiaoyan Li, Meina Kan, Shiguang Shan, and Xilin Chen. Weakly supervised object detection with segmentation collaboration. In *cvpr*, 2019. 3
- [59] Tsung-Yi Lin, Michael Maire, Serge J. Belongie, James Hays, Pietro Perona, Deva Ramanan, Piotr Dollár, and C. Lawrence Zitnick. Microsoft COCO: common objects in context. In *Proc. ECCV*, 2014. 6
- [60] Tsung-Yi Lin, Piotr Dollár, Ross Girshick, Kaiming He, Bharath Hariharan, and Serge Belongie. Feature pyramid networks for object detection. In *cvpr*, pages 2117–2125, 2017. 14
- [61] Etienne Marcheret, Gerasimos Potamianos, Josef Vopicka, and Vaibhava Goel. Detecting audio-visual synchrony using deep neural networks. In *Sixteenth Annual Conference of the International Speech Communication Association*, 2015. 2
- [62] Antoine Miech, Jean-Baptiste Alayrac, Lucas Smaira, Ivan Laptev, Josef Sivic, and Andrew Zisserman. End-to-end learning of visual representations from uncurated instructional videos. *arXiv.cs*, abs/1912.06430, 2019. 3
- [63] Pedro Morgado, Yi Li, and Nuno Vasconcelos. Learning representations from audio-visual spatial alignment. In *Proc. NeurIPS*, 2020. 3
- [64] Arsha Nagrani, Chen Sun, David Ross, Rahul Sukthankar, Cordelia Schmid, and Andrew Zisserman. Speech2action: Cross-modal supervision for action recognition. In *Proc. CVPR*, 2020. 3
- [65] Minh Hoai Nguyen, Lorenzo Torresani, Lorenzo de la Torre, and Carsten Rother. Weakly supervised discriminative localization and classification: a joint learning process. In *Proc. ICCV*, 2009. 1

- [66] Aaron van den Oord, Yazhe Li, and Oriol Vinyals. Representation learning with contrastive predictive coding. *arXiv preprint arXiv:1807.03748*, 2018. 4
- [67] Andrew Owens and Alexei A. Efros. Audio-visual scene analysis with self-supervised multisensory features. *Proc. ECCV*, 2018. 2
- [68] Andrew Owens and Alexei A. Efros. Audio-visual scene analysis with self-supervised multisensory features. In *Proc. ECCV*, 2018. 3
- [69] Andrew Owens, Phillip Isola, Josh H. McDermott, Antonio Torralba, Edward H. Adelson, and William T. Freeman. Visually indicated sounds. In *Proc. CVPR*, 2016. 2
- [70] Andrew Owens, Jiajun Wu, Josh H. McDermott, William T. Freeman, and Antonio Torralba. Ambient sound provides supervision for visual learning. In *Proc. ECCV*, 2016. 3
- [71] Mandela Patrick, Yuki M Asano, Polina Kuznetsova, Ruth Fong, João F Henriques, Geoffrey Zweig, and Andrea Vedaldi. Multi-modal self-supervision from generalized data transformations. *arXiv preprint arXiv:2003.04298*, 2020. 3, 4
- [72] A. J. Piergiovanni, Anelia Angelova, and Michael S. Ryoo. Evolving losses for unsupervised video representation learning. In *Proc. CVPR*, 2020. 3
- [73] Rui Qian, Di Hu, Heinrich Dinkel, Mengyue Wu, Ning Xu, and Weiyao Lin. Multiple sound sources localization from coarse to fine. In *Proc. ECCV*, 2020. 2
- [74] Janani Ramaswamy and Sukhendu Das. See the sound, hear the pixels. In *Proceedings of the IEEE/CVF Winter Conference on Applications of Computer Vision (WACV)*, March 2020. 2
- [75] Shaoqing Ren, Kaiming He, Ross B. Girshick, and Jian Sun. Faster R-CNN: towards real-time object detection with region proposal networks. In *arXiv:1506.01497*, 2015. 5
- [76] Shaoqing Ren, Kaiming He, Ross B. Girshick, and Jian Sun. Faster R-CNN: towards real-time object detection with region proposal networks. In *Proc. NeurIPS*, 2016. 2
- [77] Zhongzheng Ren, Zhiding Yu, Xiaodong Yang, Ming-Yu Liu, Yong Jae Lee, Alexander G. Schwing, and Jan Kautz. Instance-aware, context-focused, and memory-efficient weakly supervised object detection. In *Proc. CVPR*, 2020. 3
- [78] Zhongzheng Ren, Zhiding Yu, Xiaodong Yang, Ming-Yu Liu, Alexander G. Schwing, and Jan Kautz. UFO²: A unified framework towards omni-supervised object detection. In *Proc. ECCV*, 2020. 3
- [79] Zhongzheng Ren, Zhiding Yu, Xiaodong Yang, Ming-Yu Liu, Yong Jae Lee, Alexander G Schwing, and Jan Kautz. Instance-aware, context-focused, and memory-efficient weakly supervised object detection. In *Proceedings of the IEEE/CVF Conference on Computer Vision and Pattern Recognition*, pages 10598–10607, 2020. 14
- [80] Andrew Rouditchenko, Hang Zhao, Chuang Gan, Josh McDermott, and Antonio Torralba. Self-supervised audio-visual co-segmentation. In *Proc. ICASSP*, pages 2357–2361. IEEE, 2019. 2
- [81] Ramprasaath R Selvaraju, Michael Cogswell, Abhishek Das, Ramakrishna Vedantam, Devi Parikh, and Dhruv Batra. Grad-cam: Visual explanations from deep networks via gradient-based localization. In *Proceedings of the IEEE international conference on computer vision*, pages 618–626, 2017. 2, 3
- [82] Arda Senocak, Tae-Hyun Oh, Junsik Kim, Ming-Hsuan Yang, and In So Kweon. Learning to localize sound source in visual scenes. In *Proc. CVPR*, 2018. 2, 7
- [83] Y. Shen, R. Ji, Y. Wang, Y. Wu, and L. Cao. Cyclic guidance for weakly supervised joint detection and segmentation. In *2019 IEEE/CVF Conference on Computer Vision and Pattern Recognition (CVPR)*, pages 697–707, 2019. 3
- [84] Y. Shen, R. Ji, S. Zhang, W. Zuo, and Y. Wang. Generative adversarial learning towards fast weakly supervised detection. In *2018 IEEE/CVF Conference on Computer Vision and Pattern Recognition*, pages 5764–5773, 2018. 3
- [85] Krishna Kumar Singh and Yong Jae Lee. Hide-and-seek: Forcing a network to be meticulous for weakly-supervised object and action localization. In *2017 IEEE international conference on computer vision (ICCV)*, pages 3544–3553. IEEE, 2017. 3
- [86] Krishna Kumar Singh and Yong Jae Lee. You reap what you sow: Using videos to generate high precision object proposals for weakly-supervised object detection. In *CVPR*, 2019. 3
- [87] Chen Sun, Fabien Baradel, Kevin Murphy, and Cordelia Schmid. Contrastive bidirectional transformer for temporal representation learning. *arXiv.cs*, abs/1906.05743, 2019. 3
- [88] Chen Sun, Austin Myers, Carl Vondrick, Kevin Murphy, and Cordelia Schmid. Videobert: A joint model for video and language representation learning. In *Proc. ICCV*, 2019. 3
- [89] Peng Tang, Xinggang Wang, Song Bai, Wei Shen, Xiang Bai, Wenyu Liu, and Alan Yuille. Pcl: Proposal cluster learning for weakly supervised object detection. *IEEE transactions on pattern analysis and machine intelligence*, 42(1):176–191, 2018. 6
- [90] Peng Tang, Xinggang Wang, Song Bai, Wei Shen, Xiang Bai, Wenyu Liu, and Alan L. Yuille. PCL: proposal cluster learning for weakly supervised object detection. *CoRR*, abs/1807.03342, 2018. 3, 6, 7
- [91] Peng Tang, Xinggang Wang, Xiang Bai, and Wenyu Liu. Multiple instance detection network with online instance classifier refinement. In *Proc. CVPR*, 2017. 3
- [92] Yonglong Tian, Dilip Krishnan, and Phillip Isola. Contrastive multiview coding. *arXiv preprint arXiv:1906.05849*, 2019. 3
- [93] Yapeng Tian, Jing Shi, Bochen Li, Zhiyao Duan, and Chenliang Xu. Audio-visual event localization in unconstrained videos. In *Proc. ECCV*, 2018. 3
- [94] J.R.R. Uijlings, K.E.A. van de Sande, T. Gevers, and A.W.M. Smeulders. Selective search for object recognition. *International Journal of Computer Vision*, 2013. 7
- [95] Wouter Van Gansbeke, Simon Vandenhende, Stamatios Georgoulis, Marc Proesmans, and Luc Van Gool. Scan: Learning to classify images without labels. In *European Conference on Computer Vision (ECCV)*, 2020. 2
- [96] Wouter Van Gansbeke, Simon Vandenhende, Stamatios Georgoulis, Marc Proesmans, and Luc Van Gool. Scan: Learning to classify images without labels. In *Proceedings of the European Conference on Computer Vision*, 2020. 6
- [97] Wouter Van Gansbeke, Simon Vandenhende, Stamatios

- Georgoulis, and Luc Van Gool. Unsupervised semantic segmentation by contrasting object mask proposals. *arxiv preprint arxiv:2102.06191*, 2021. 2
- [98] Fang Wan, Chang Liu, Wei Ke, Xiangyang Ji, Jianbin Jiao, and Qixiang Ye. C-mil: Continuation multiple instance learning for weakly supervised object detection. In *cvpr*, 2019. 3
- [99] Xiaolong Wang, Abhinav Shrivastava, and Abhinav Gupta. A-Fast-RCNN: Hard positive generation via adversary for object detection. In *Proc. CVPR*, 2017. 3
- [100] Zhirong Wu, Yuanjun Xiong, Stella X. Yu, and Dahua Lin. Unsupervised feature learning via non-parametric instance discrimination. In *Proc. CVPR*, 2018. 1
- [101] Junyuan Xie, Ross Girshick, and Ali Farhadi. Unsupervised deep embedding for clustering analysis. In *International conference on machine learning*, pages 478–487, 2016. 2
- [102] G. Yan, B. Liu, N. Guo, X. Ye, F. Wan, H. You, and D. Fan. C-midn: Coupled multiple instance detection network with segmentation guidance for weakly supervised object detection. In *2019 IEEE/CVF International Conference on Computer Vision (ICCV)*, pages 9833–9842, 2019. 3
- [103] Jianwei Yang, Devi Parikh, and Dhruv Batra. Joint unsupervised learning of deep representations and image clusters. In *CVPR*, pages 5147–5156, 2016. 2
- [104] Zhenheng Yang, Dhruv Mahajan, Deepti Ghadiyaram, Ram Nevatia, and Vignesh Ramanathan. Activity driven weakly supervised object detection. In *cvpr*, 2019. 3
- [105] Zhaoyang Zeng, Bei Liu, Jianlong Fu, Hongyang Chao, and Lei Zhang. Wsod2: Learning bottom-up and top-down objectness distillation for weakly-supervised object detection. In *iccv*, 2019. 3
- [106] Xiaopeng Zhang, Jiashi Feng, Hongkai Xiong, and Qi Tian. Zigzag learning for weakly supervised object detection. In *CVPR*, 2018. 3
- [107] Y. Zhang, Y. Bai, M. Ding, Y. Li, and B. Ghanem. W2f: A weakly-supervised to fully-supervised framework for object detection. In *2018 IEEE/CVF Conference on Computer Vision and Pattern Recognition*, pages 928–936, 2018. 3
- [108] Hang Zhao, Chuang Gan, Wei-Chiu Ma, and Antonio Torralba. The sound of motions. *Proc. ICCV*, 2019. 2, 3
- [109] Hang Zhao, Chuang Gan, Andrew Rouditchenko, Carl Vondrick, Josh McDermott, and Antonio Torralba. The sound of pixels. In *Proc. ECCV*, 2018. 2, 7
- [110] M. Zhao, T. Li, M. A. Alsheikh, Y. Tian, H. Zhao, A. Torralba, and D. Katabi. Through-wall human pose estimation using radio signals. In *2018 IEEE/CVF Conference on Computer Vision and Pattern Recognition*, pages 7356–7365, 2018. 3
- [111] Bolei Zhou, Aditya Khosla, Àgata Lapedriza, Aude Oliva, and Antonio Torralba. Learning deep features for discriminative localization. In *CVPR*, 2016. 3, 5
- [112] Yang Zou, Zhiding Yu, Xiaofeng Liu, B. V. K. Vijaya Kumar, and Jinsong Wang. Confidence regularized self-training. In *Proc. ICCV*, 2019. 3

Appendix

This Appendix provides: additional qualitative results including failure analysis (Sec. A), further implementation details (Sec. B) and label mapping details (Sec. C).

A. Qualitative analysis & failure cases

In Figure A.1 we show more qualitative results for the general object detection experiment. In Figure A.2 we show some more examples of our trained detector’s output on detecting musical instruments on the OpenImages test set, including failure cases. As noted in the main paper, the model’s detections are very precise, especially for visually distinct categories such as Accordion, Harp, Cello etc.

The failure cases can be attributed to either incorrect box predictions or misclassifications. Box-prediction failure modes most commonly manifest as i) grouping multiple instances into the same detection, ii) missing instances or iii) detection of only parts of an object. All those issues are common and well documented in the WSOD literature [79]. We observe that in the case of objects that appear with high granularity – e.g. drums – although qualitatively the detections seem reasonable, the multiple instance grouping problem is prominent; this explains our model’s low performance by quantitative measures (mAP) for these classes.

Another error is detecting parts of wrong objects that often appear together with the objects of interest due to biases in the data. For example sometimes mouth regions are detected as wind instruments. This is expected when using the audio-visual correspondence as the training signal.

Wrong classification on the other hand occurs often because i) visually similar classes are confused - e.g. Saxophone and Oboe, Horn and Trumpet; ii) of incorrect cluster-to-ground-truth-label matching, e.g. cluster with high Trombone purity matched to Horn; iii) sometimes the model confuses the class due to the object’s orientation – for example a vertical violin is detected as a cello or vice versa a horizontal cello is detected as violin.

B. Additional implementation details

Visual & audio encoder architecture. For the visual and audio encoders (q^v, q^a) we use the AVOL-Net [7] architecture. Each network is a 8-layer CNN with an architecture similar to VGG-M. For a typical $224 \times 224 \times 3$ RGB image input, the video encoder outputs a 14×14 visual feature map. The inputs to the audio encoder are 257×200 dimensional log-mel spectrograms, extracted from 1 second of audio sampled at 24Hz. The output of the encoder is average pooled, resulting in a single audio feature vector.

Localisation and classification heads. As localisation $f^{\{v,a\}}$ and classifier $g^{\{v,a\}}$ networks we use for each modality a 2-layer MLP with a hidden dimension of 512.

The MLPs do not share weights and are applied on top of the common representations extracted by the video and audio encoders. The visual feature maps are average-pooled before being input to the classification network g^v , while f^v is applied directly on the spatial feature map, as discussed in Section 3.1 of the main paper. The output dimension for the localisation networks (i.e. the common embedding dimension) is 128, while the audio and video classifier heads each output K values, one for every cluster.

Detector backbone. As the backbone for the Faster R-CNN detector we use a ResNet50(1x) [22, 41] model pre-trained without labels using the SimCLR [22] method on ImageNet. We use the pretrained weights¹ released by the authors of [22]. We apply a Feature Pyramid Network (FPN) [60] on top of the activations of different backbone layers extracting visual features at five spatial scales, i.e. $/4, /8, /16, /32, \text{ and } /64$ of the input resolution. Feature descriptors are extracted for every proposal with ROI-align pooling [40].

Detector RPN training. The box proposals $m \in M(v)$ used by the Faster R-CNN detector are produced by a Region Proposal Network (RPN). The RPN extracts a set of anchors $n \in N(v) \subset \Omega^2$ at three aspect ratios (0.5, 1.0 and 1.5) on each FPN output scale. The extracted number of anchors depends only on the input image dimensions.

The RPN contains 2 MLP heads in order to model $o(n) = f_{\text{rpn}}^{\text{obj}}(n|v) \in \{0, 1\}$, a binary objectness label indicating whether anchor n contains an object or background, and $m(n) = f_{\text{rpn}}^{\text{loc}}(n|v) \in \mathbb{R}^4$, the bounding box proposal resulting from anchor n .

The RPN heads are trained jointly with the detector heads, using the input box annotations and ignoring the class labels: if $n^* = \arg \max_{n \in N(v)} \text{IoU}(n, t^*)$ is the anchor that matches the pseudo-ground truth bounding box t^* the best, one optimizes:

$$\mathcal{L}_{\text{rpn}}(v, t^*) = \mathcal{L}_{\text{reg}}(m(n^*), t^*) + \mathcal{L}_{\text{obj}}(o(n^*), 1) + \sum_{a \in A(v): \text{IoU}(n, t^*) < \tau} \mathcal{L}_{\text{obj}}(o(n), 0).$$

Here \mathcal{L}_{reg} is the L^1 loss for the bounding box corner coordinates and \mathcal{L}_{obj} a binary cross-entropy loss. Similarly to the detector loss, the RPN loss requires the best anchor n^* to match bounding box t^* and to have a high objectness score, while reducing the objectness scores of anchors n that are a bad match.

Training details. For all the experiments we pre-train the video and audio backbones using the localisation objective only and average-pooling instead of max-pooling on the heatmap. The pre-training is performed on the Audioset-Instruments training set for 230 epochs on 64 GPUs with a

¹<https://github.com/google-research/simclr>

VGGSound label (representative)	OpenImages label (test)
airplane flyby	Airplane
ambulance siren	Ambulance
mynah bird singing	Bird
racing car	Car
cat purring	Cat
typing on computer keyboard	Computer Keyboard
mouse clicking	Computer Mouse
frog croaking	Frog
helicopter	Helicopter
lions roaring	Lion
driving snowmobile	Snowmobile

Table A.1: Mapping of VGGsound to OpenImages labels for qualitative evaluation on non-instrument object categories shown in Figure A.1.

batch size of 12 per GPU, using the Adam optimizer with a constant learning rate of 6.4×10^{-4} and standard hyperparameters. The learning rate is initially set to 1×10^{-5} and warmed up gradually until reaching the constant value after 10 epochs. The joint localisation and clustering training is performed on 16 GPUs with a batch size of 16 per GPU and SGD optimization with a constant learning rate of 0.005 and momentum 0.9, for a further 300 epochs. We set hyperparameter λ to 0.5. The temperature for the contrastive learning is learned as a single scalar weight. The detector training is performed on 16 GPUs with a batch size of 12, SGD optimization and learning rate 0.008 for 100 epochs. The total training takes approximately 3 days in this setting.

C. Additional label mapping details

In Table A.2 we show the full list of VGGSound video categories used for training our models. We use only samples from the 39 *mappable* classes for the detector training stage if not stated otherwise.

The 15 *test* labels shown are the musical instrument labels found in the OpenImages dataset. As explained in the main paper, the Audioset and VGGSound test sets that we use for evaluation have been pseudo-labelled with high confidence detections from a supervised detector trained on OpenImages by [30], therefore these 15 test labels are common among all our test sets.

We use the same colour to show the manual grouping of VGGSound labels that we use for some of the baseline and ablation experiments. The many-to-one grouping of the *mappable* into *representative* labels is used for training the PCL WSOD baseline and also for evaluating the “manual” matching strategy in Table 6 of the main paper. We note that our proposed method **does not** use this mapping, but instead

uses the Hungarian algorithm for matching our learned clusters directly to the *representative* classes. On the same table we also show the constant mapping of *representative* VGGSound labels to the OpenImages test labels that is necessary for evaluation. The majority of the instrument categories are matched exactly, except for the ‘Guitar’ and ‘Drum’ test labels for which we had to choose one of the candidates from the VGGSound guitar and drum subsets; we chose “playing electric guitar” and “playing snare drum” as the representative labels respectively. Note that since the Hungarian matching only matches one cluster to every test label, only choosing one *representative* class, harms our detectors, which are in fact more specialised. For example instances of acoustic guitar that may be correctly detected and not labelled as electric guitar will not be taken into account, in effect lowering our method’s measured performance.

Similarly in Table A.1 we show the *representative* to *test* mapping used for evaluation and visualisation in the non-instrument object detection experiment.

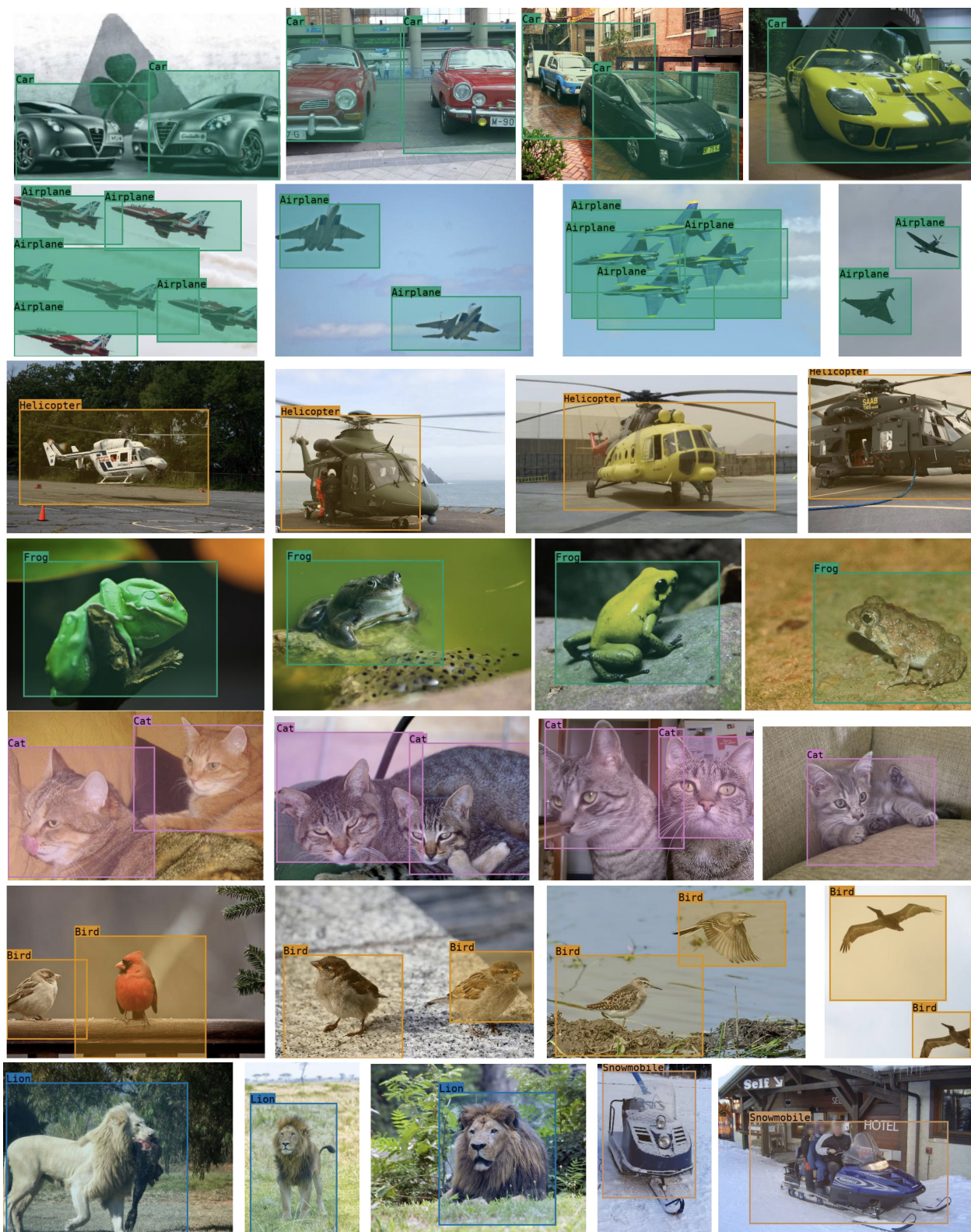


Figure A.1: **Object detection beyond musical instruments.** Our proposed method can learn to accurately detect objects from more general categories, as long as they can be associated with a characteristic sound. The results shown here are from a model trained without labels directly on the full VGGSound dataset which includes 309 different video classes.

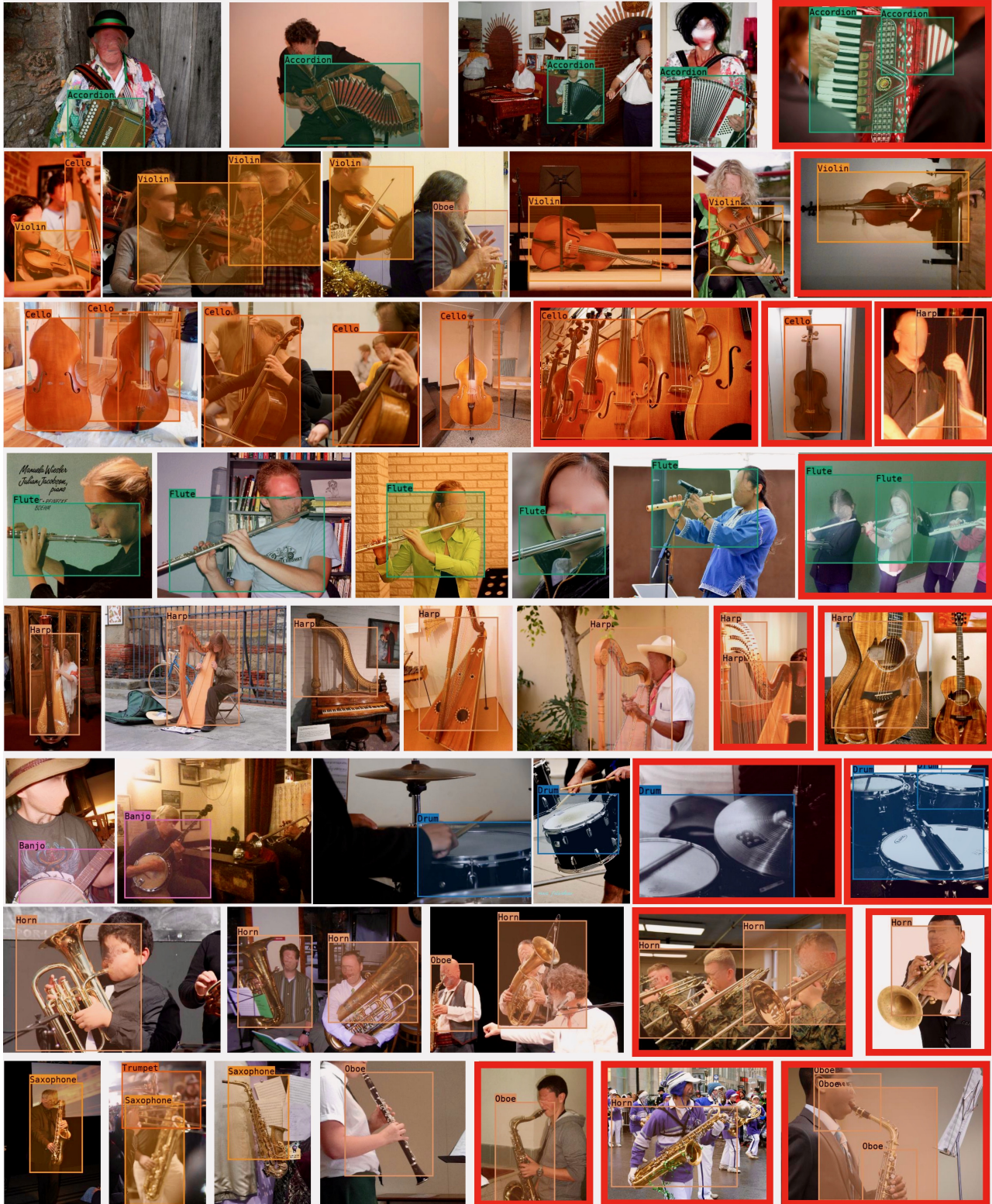


Figure A.2: Additional qualitative examples and failure cases. The images highlighted in red contain failure cases.

VGGS instrument classes (50)	mappable (39)	representative (15)	test (15)
playing accordion	playing accordion	playing accordion	Accordion
playing double bass	playing double bass	playing cello	Cello
playing bassoon	playing bassoon	playing flute	Flute
playing cello	playing cello	playing electric guitar	Guitar
playing clarinet	playing clarinet	playing harp	Harp
playing cornet	playing cornet	playing oboe	Oboe
playing flute	playing flute	playing piano	Piano
playing acoustic guitar	playing acoustic guitar	playing saxophone	Saxophone
playing bass guitar	playing bass guitar	playing trombone	Trombone
playing electric guitar	playing electric guitar	playing trumpet	Trumpet
tapping guitar	tapping guitar	playing violin	Violin
playing harp	playing harp	playing banjo	Banjo
playing harpsichord	playing harpsichord	playing harmonica	Harmonica
playing oboe	playing oboe	playing french horn	Horn
playing electronic organ	playing electronic organ	playing snare drum	Drum
playing hammond organ	playing hammond organ		
playing piano	playing piano		
playing saxophone	playing saxophone		
playing trombone	playing trombone		
playing trumpet	playing trumpet		
playing ukulele	playing ukulele		
playing violin	playing violin		
playing mandolin	playing mandolin		
playing banjo	playing banjo		
playing harmonica	playing harmonica		
playing french horn	playing french horn		
playing drum kit	playing drum kit		
playing bass drum	playing bass drum		
playing snare drum	playing snare drum		
playing tabla	playing tabla		
playing bongo	playing bongo		
playing tambourine	playing tambourine		
playing timpani	playing timpani		
playing tympani	playing tympani		
playing timbales	playing timbales		
playing congas	playing congas		
playing djembe	playing djembe		
playing cymbal	playing cymbal		
playing gong	playing gong		
playing didgeridoo			
playing bugle			
playing shofar			
playing glockenspiel			
playing vibraphone			
playing marimba			
playing bagpipes			
playing theremin			
playing steel guitar			
playing sitar			
playing erhu			

Table A.2: **VGGSound instrument categories and labels mapping**. The 15 *test* labels are the OpenImages instrument labels that all our tests sets are labelled with. The 39 *mappable* labels comprise the VGGSound subset that can be roughly mapped to those 15 test labels – this mapping is necessary for evaluation. The *representative* classes are the ones that we use to link VGGSound labels with the 15 test labels for evaluation. Labels manually matched by us are shown with the same colour.